

DECOMPOSITION OF NO STUDIED BY INFRARED
EMISSION AND CO LASER ABSORPTION

R. K. Hanson, W. L. Flower, J. P. Monat and C. H. Kruger
Mechanical Engineering Department
Stanford University, U.S.A.

ABSTRACT

A diagnostic technique for monitoring the concentration of NO using absorption of CO laser radiation has been developed and applied in a study of the decomposition kinetics of NO. Simultaneous measurements of infrared emission by NO at 5.3 microns were also made to validate the laser absorption technique. The data were obtained behind incident shocks in NO-N₂O-Ar (or Kr) mixtures, with temperatures in the range 2400-4100°K. Rate constants for dominant reactions were inferred from comparisons with computer simulations of the reactive flow.

INTRODUCTION

The anticipated availability of tunable continuous-wave infrared lasers offers prospects for important new quantitative spectroscopic techniques well suited for shock tube kinetics studies of infrared-active gases. One obvious advantage of tunable laser spectroscopy is high specificity for a given chemical compound so that negligible interference is produced by other constituents present in a mixture.

To investigate the potential of tunable lasers for shock tube applications we have constructed a discretely tunable CO laser and used it for absorption measurements of NO, taking advantage of the near-coincidence of some NO vibration-rotation absorption lines and CO gas laser lines (refs. 1, 2). In this paper we describe the experimental apparatus and compare simultaneous measurements of NO concentration obtained using laser absorption and infrared emission techniques. Some results for rate coefficients relevant to NO decomposition kinetics are also presented.

EXPERIMENTAL

The experiments were done behind incident shock waves in a conventional, pressure-driven shock tube (15-cm internal diameter). Shock speeds varied from about 1.3 to 1.8 mm/ μ sec, producing frozen-chemistry temperatures of 2500-4100°K and postshock pressures between 0.3 and 0.5 atmospheres. Test gases consisted of NO in an excess of either Ar or Kr, with a trace amount of N₂O added in some experiments. The mixtures were prepared manometrically and mixed immediately before each run.

A schematic of the experimental setup is shown in Fig. 1. The CO laser was operated on a single vibration-rotation line at $\nu=1935.48$ cm⁻¹ ($V=7 \rightarrow 6$, $J=12 \rightarrow 13$) with a typical output power of about 0.1 W. The absorption line of NO is centered at $\nu=1935.49$ cm⁻¹ ($^2\Pi_{3/2}$, $V=0$, $m=39/2$) (ref. 1). Transmitted radiation is directed onto a photovoltaic InSb detector (liquid-nitrogen cooled). The data is displayed on an oscillogram, as shown in Fig. 2a. The data displayed include the transmitted intensity $I(t)$, the zero signal (laser blocked off), and the absorption $I_0 - I(t)$, where t is the time after shock arrival.

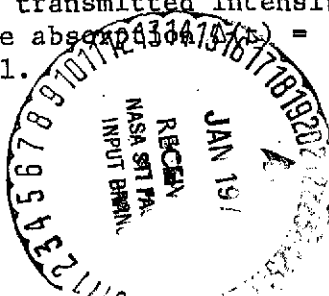
(NASA-CR-141275) DECOMPOSITION OF NO
STUDIED BY INFRARED EMISSION AND CO LASER
ABSORPTION (Stanford Univ.) 4 p HC \$3.25

CSCS 13B

G3/45

Unclass
06560

N75-15197



The governing equation for absorption is the Beer-Lambert Law

$$I = I_0 \exp(-\beta L[NO]) \quad (1)$$

where I_0 and I are the incident and transmitted light fluxes and L is the path length of the beam through the sample. The absorption coefficient β is a function of temperature, pressure and composition and is essentially zero before the shock arrives. For the small absorptions to be reported here, the absorption is given approximately by

$$\Delta(t)/\Delta^* = \beta[NO]/(\beta[NO])^* \approx [NO]/[NO]^* \quad (2)$$

where the asterisk denotes some convenient reference condition. Here we have elected to neglect the small changes in β which occur on the time scale of interest after the shock. Thus, for present purposes we can plot Δ/Δ^* and compare this directly with calculations of $[NO]/[NO]^*$.

The infrared emission system has been described previously (refs. 3,4). The emission from the fundamental vibration-rotation band of NO (at 5.3 microns) is isolated from N₂O emission (4.5-micron band) using a filter passing wavelengths greater than 5.0 microns. The detector is coupled to an amplifier whose output is displayed on an oscilloscope. A typical record is shown in Fig. 2b.

For an ideal system, the output voltage of the amplifier V is proportional to the intensity of spontaneous emission I , which in turn is proportional for an optically thin gas to the product of the NO concentration and the vibrational energy per unit concentration of NO, $e_v(T)$. For the present we choose to neglect the influence of small temperature changes so that V is linearly proportional to $[NO]$ and we may conveniently plot

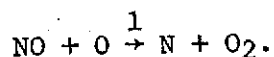
$$V/V^* = [NO]/[NO]^* \quad (3)$$

for comparison with both the laser absorption data and computer calculations of the reacting flow.

RESULTS

Results based on the data of Fig. 2 are presented in Fig. 3. Here we have plotted absorption and emission data and kinetic calculations of $[NO]/[NO]_{\max}$, the maximum NO concentration providing a convenient reference for normalization of the calculations and the absorption data. Because of initial formation of additional NO during the decomposition of N₂O, the peak value of $[NO]$ occurs about 1 μ sec after shock arrival. Unfortunately, the emission data at 1 μ sec is distorted by two nonideal effects, NO vibrational relaxation and a slight transient interference from N₂O emission. To minimize these effects, we have normalized the emission data to match the kinetic calculations at 5 μ sec.

Kinetic calculations were made with the NASA Lewis Kinetics Program (ref. 5) using a nine-reaction scheme developed in a previous study (ref. 3). After the rapid decomposition of the initial N₂O, the rate-limiting step for NO removal is the reaction



The N_2O was added in many of the experiments to serve as a quick source of oxygen atoms, thereby enhancing the role of reaction 1 in the overall NO decomposition scheme. The calculated NO profile shown in Fig. 3 was obtained by choosing the value of k_1 so as to yield the best fit to the data. All other rate constants were held fixed. Calculations testing sensitivity to reasonable variations in other rate constants substantiated this approach for present conditions. Results for k_1 and other rate constants inferred from fits to the data from all the experiments will be presented in the complete paper.

The good agreement in Fig. 3 between the two independent measurements of [NO] serves to validate the laser absorption technique and also provides some indication of the accuracy with which [NO] can be determined using these methods. The interference in the NO emission data due to N_2O emission, even in this relatively simple mixture and with a carefully chosen filter, emphasizes the merit of tunable laser spectroscopy.

Measured values for the absorption coefficient β were in the range $5-11 \times 10^4 \text{ cm}^2/\text{mole}$, decreasing with increasing temperature. Detailed results will be presented in the full paper.

We gratefully acknowledge support of this work by the National Science Foundation and the National Aeronautics and Space Administration.

REFERENCES

1. C. Chackerian, Jr. and M. F. Weisbach, Opt. Soc. America **63**, 342 (1973).
2. R. T. Menzies, App. Optics **10**, 1532 (1971).
3. R. K. Hanson, W. L. Flower and C. H. Kruger, Comb. Sci. and Tech., Dec. 1974 (in press).
4. W. L. Flower, R. K. Hanson and C. H. Kruger, 15th Symp. (Intern.) on Combustion (Tokyo, 1974).
5. D. A. Bittker and V. J. Scullin, NASA TN D-6586 (1972).

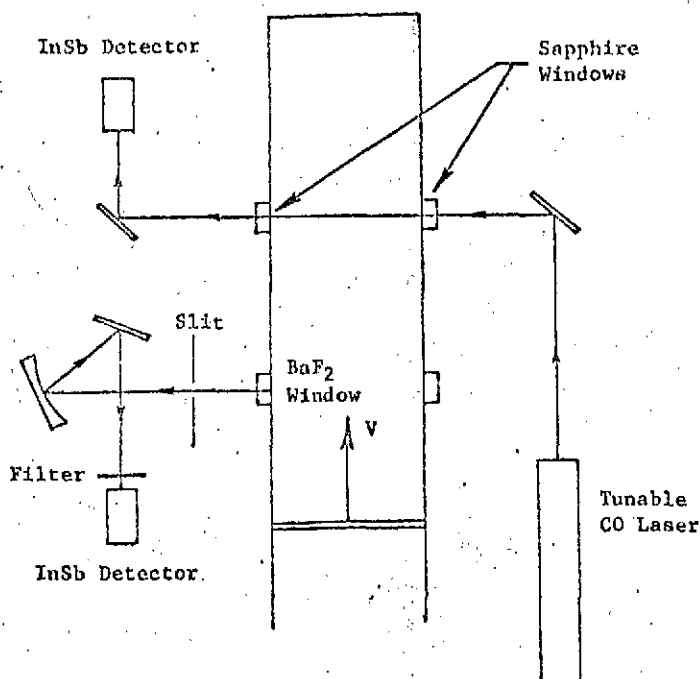


Fig. 1 Schematic of experiment.

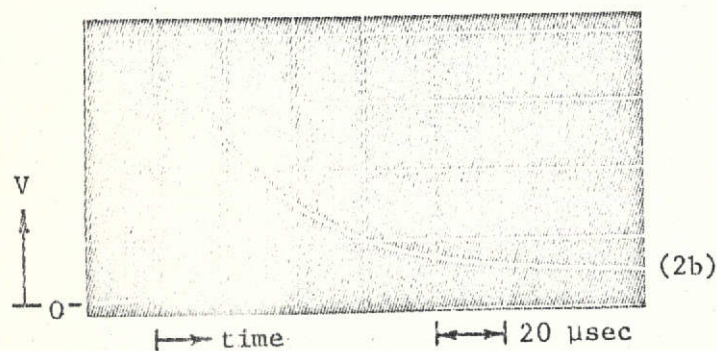
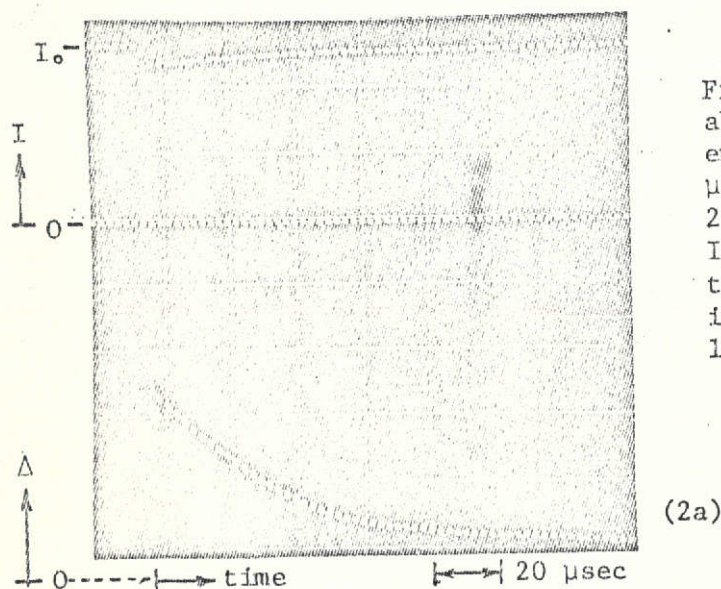


Fig.2 Typical data: CO laser absorption (Fig. 2a) and NO IR emission (Fig. 2b). $V=1.53\text{mm}/\mu\text{sec}$, $P_1=6.94\text{ Torr}$ ($\text{N}_2\text{O}/\text{NO}/\text{Kr} = 2.2/9.8/88$), $T_{2\text{frozen}} = 4048^\circ\text{K}$. In Fig. 2a the vertical sensitivities are 50 and $5\text{mV}/\text{div}$; in Fig. 2b the sensitivity is $10\text{mV}/\text{div}$.

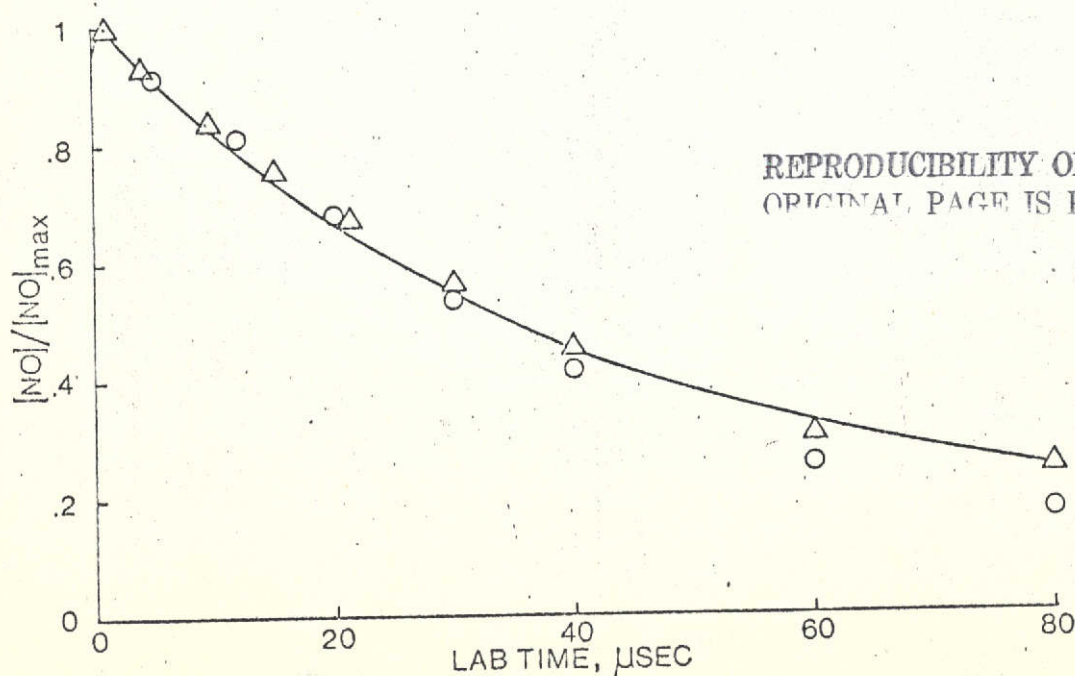


Fig.3 Absorption and emission data and kinetic calculations of $[\text{NO}]/[\text{NO}]_{\text{max}}$. Shock conditions are the same as Fig.2: —, Kinetic calculations with $k_1 = 2.7 \times 10^9 T \exp(-38640/RT) \text{ cm}^3/\text{mol-s}$; Δ , absorption data for $\Delta(t)/\Delta_{\text{max}}$; \circ , emission data for V/V_{max} renormalized to match kinetic calculations at $5\text{ }\mu\text{sec}$.